

Journal of Materials Chemistry A

Accepted Manuscript



This is an *Accepted Manuscript*, which has been through the Royal Society of Chemistry peer review process and has been accepted for publication.

Accepted Manuscripts are published online shortly after acceptance, before technical editing, formatting and proof reading. Using this free service, authors can make their results available to the community, in citable form, before we publish the edited article. We will replace this *Accepted Manuscript* with the edited and formatted *Advance Article* as soon as it is available.

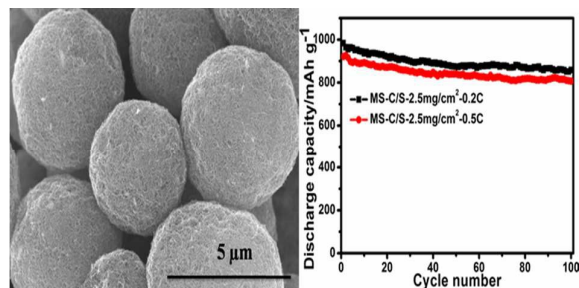
You can find more information about *Accepted Manuscripts* in the [Information for Authors](#).

Please note that technical editing may introduce minor changes to the text and/or graphics, which may alter content. The journal's standard [Terms & Conditions](#) and the [Ethical guidelines](#) still apply. In no event shall the Royal Society of Chemistry be held responsible for any errors or omissions in this *Accepted Manuscript* or any consequences arising from the use of any information it contains.

A novel type of MWCNTs microspheres was synthesized and applied to the sulfur cathode of high performance lithium-sulfur batteries.

MWCNTs porous microspheres with efficient 3D conductive network for high performance lithium-sulfur batteries

Xiaomin Ye,^{†a,b} Jie Ma,^{†b} Yongsheng Hu,^{*b} Huiying Wei^{*a} and Fangfu Ye^{*b}



A novel multi-walled carbon nanotubes microspheres were successfully prepared and applied to the sulfur cathode of lithium sulfur batteries.

MWCNTs porous microspheres with efficient 3D conductive network for high performance lithium-sulfur batteries

Xiaomin Ye,^{‡a,b} Jie Ma,^{‡b} Yong-sheng Hu,^{*b} Huiying Wei^{*a} and Fangfu Ye^{*b}

a. Key Laboratory for Special Functional Aggregate Materials of Education Ministry, School of Chemistry and Chemical Engineering, Shandong University, Jinan 250100, China. E-mail: weihuiying@sdu.edu.cn; Fax: +86-531-88564464; Tel: +86-531-88365431

b. Key Laboratory for Renewable Energy, Beijing Key Laboratory for New Energy Materials and Devices, National Laboratory for Condensed Matter Physics, Institute of Physics, Chinese Academy of Sciences, Beijing 100190, China. E-mail: yshu@aphy.iphy.ac.cn

[†]Electronic Supplementary Information (ESI) available: [details of any supplementary information available should be included here]. See DOI: 10.1039/x0xx00000x

[‡] X. M. Ye and J. Ma contributed equally to this work.

Abstract

Lithium-sulfur (Li-S) batteries are considered as a promising commercial alternative to lithium-ion batteries (LIBs) for next-generation battery systems. However, the practical application of Li-S batteries is hindered by several obstacles, such as the insulating nature of elemental sulfur and the high solubility of the lithium polysulfide products. In this work, a new type of multi-walled carbon nanotubes (MWCNTs) microspheres was synthesized successfully and used as a carbon framework for sulfur cathode of lithium sulfur batteries. Commercial aqueous-dispersed MWCNTs of low cost are an easy access for large-scale production of the carbon skeleton through a simple spray drying approach. The as-prepared carbon framework shows a porous microspherical architecture with particle size around several micrometers, and the MWCNTs in it are intertwined to construct a three-dimensional (3D) continuous electronic conductive network. For the sulfur cathode, the C/S microspheres (MS-C/S) was facily prepared by a melt-diffusion way. The obtained MS-C/S electrode displays excellent cycling stability and rate capability. The electrode with a sulfur loading of 2.5 mg cm⁻² shows an initial discharge capacity of 983 mA h g⁻¹ and a stable capacity of 858 mA h g⁻¹ after 100 cycles at a current rate of 0.2 C. Even the current rate increases to 0.5 C, a stable capacity of 806 mA h g⁻¹ is maintained over 100 cycles.

Introduction

With the development of high performance portable electric devices, electric vehicles and energy storage systems, lithium rechargeable batteries require increasingly high power and energy density. However, traditional lithium-ion batteries (LIBs) are approaching the theoretical energy density limit.¹⁻⁴ For example, LiCoO₂ and LiNi_{1/3}Co_{1/3}Mn_{1/3}O₂, the common cathode materials for LIBs, have a restricted gravimetric energy density of less than 300 Wh/kg, which is not sufficient to satisfy the increasing requirement for the emerging market. Thus, it is urgent to explore new electrode materials or new battery systems.⁵⁻⁹

In this regard, lithium-sulfur (Li-S) batteries, which possess a theoretical capacity of 1672 mA h g⁻¹, are one of the most promising candidates for next-generation battery systems.¹⁰⁻¹² The sulfur based cathode material has advantages of natural abundance, low environmental impact and low cost. However, the practical application of Li-S batteries is hindered by several obstacles. One is the insulating nature of the element sulfur (~5 × 10⁻³⁰ S/cm at room temperature), which leads to the low utilization of the active material, severe capacity fading and poor cycle stability.¹³⁻¹⁸ Furthermore, the high solubility of the lithium

polysulfide products (Li_2S_x , $x > 2$) in organic electrolyte results in significant morphology and component changes in the electrode.¹⁹⁻²⁴ In addition, the large volumetric change ($\sim 80\%$) of sulfur during Li insertion and extraction processes deteriorates the mechanical integrity and stability of the electrode over cycles.^{25, 26}

Over the past few decades, considerable researches have focused on developing methods to overcome these drawbacks by introducing conductive agents with special structures. For example, efforts have been made to prepare structurally and morphologically different carbon support materials, including mesoporous carbon,²⁷ graphene,²⁸ microporous carbon,²⁹ carbon nanofibers³⁰ and carbon nanotubes,^{31, 32} which have been composited with sulfur by various methods to improve the capacity and cycle stability of sulfur cathodes. Chen et al. reported a graphene-based three-dimensional hierarchical sandwich-type architecture, which exhibits a high initial capacity of 1396 mA h g^{-1} at the current density of 0.2 C. The synergistic effect of graphene sheets and MWCNTs within the C/S nanocomposite provides a good conductive network for electron transport, a strong confinement for soluble polysulfide as well as an effective buffer for volume expansion of the sulfur cathode during discharge.³³ MWCNTs own high conductivity and a unique structure with high aspect ratio, and thus provide a fast electron diffusion pathway. It was reported that MWCNTs could improve the long time cycle performance of Li-S batteries.¹³ Guo et al. synthesized disordered carbon nanotubes for the carbon framework of the sulfur cathode by using a template wetting technique based on commercial anodic aluminum oxide membranes.³⁴ The as-prepared samples heated at 500°C show the best electrochemical performance of $\sim 670 \text{ mA h g}^{-1}$ at 0.25 C after 100 cycles. However, the preparation process is very complicated. There are many disadvantages of using carbon nanotubes (CNTs) as carbon support material. Firstly, CNTs tend to agglomerate because of van der Waals interactions, which limits their efficiency as sulfur hosts; secondly, the conductivity of one-dimensional materials is worse than that of three-dimensional materials; thirdly, practical large-scale synthesis of carbon frameworks based on CNTs with homogenous architecture remains challenging. In addition, nano-size materials show much lower tap density than micro-size materials.

In this article we report a large-scale synthesis of carbon frameworks composed of MWCNTs porous microspheres (MS-C) through a spray drying method, which is widely used for spherical shape granulating in industry and has been used in our previous work to synthesize a C/S nanocomposite.³⁵ The aqueous-dispersed MWCNTs with low cost, are commercially available. The MS-C has a homogeneous porous microspherical morphology with particle size of several micrometers. We then use a melt-diffusion method to obtain carbon/sulfur microspheres (MS-C/S) with the same microspherical structure and apply them to Li-S batteries. The MS-C/S cathode delivers an initial capacity of 983 mA h g^{-1} and a stable capacity of 858 mA h g^{-1} over 100 cycles at 0.2 C. Even at 0.5 C, a capacity of 808 mA h g^{-1} after 100 cycles can be obtained. Such an excellent rate capability and cycle stability are attributed to the carbon frameworks, which possess an interconnective polyporous microspherical architecture and offers effective 3D conductive networks for electron transport and ion diffusion, strong immobilization of soluble polysulfide, and mechanical support for volume expansion/shrinkage of the sulfur cathode during the charge/discharge process.

Experiment

Chemicals and Materials

Sublimed sulfur (S, 99.5%, Alfa Aesar), carbon disulfide (CS₂, AR, Shanghaihushi), MWCNTs (CNano Technology Company, TM-9000), MWCNTs aqueous dispersion (CNano Technology Company, LB200), dimethoxy ethane (DME) and 1,3-dioxolane (DOL) (2:1 V/V, BASF), lithium bis (trifluoromethane sulphonyl) imide (LiN(SO₂CF₃)₂, LiTFSI, TCI, Japan), lithium nitrate (LiNO₃, 99+%, Alfa Aesar), ammonium bicarbonate (NH₄HCO₃, AR, Shanghaihushi), commercial Ketjenblack (KB, Shanghai Tengmin Industry Company, EC300J), sodium carboxymethyl cellulose (CMC) and styrene-butadiene rubber (SBR) were obtained from commercial sources. All chemicals and materials were used without any further treatment.

Carbon/Sulfur microspheres Preparation

First, the MWCNTs aqueous dispersion was diluted with the same volume of distilled water, and the diluted dispersion was spray-dried at 130 °C to obtain porous microspheres. Then, sulfur (1.4 g) and the prepared MWCNTs microspheres (0.6 g) were added into carbon disulfide (15 mL) by stirring for 1 h. Carbon disulfide was evaporated and recycled by rotary evaporation. At last, the mixture was sealed in a glass tube and heated at 155 °C for 12 h.

For comparison, we also prepare a control sample. We grinded sulfur and pure MWCNTs for 30 minutes and then heat them at 155 °C for 12 h. For convenience, we will use the abbreviation T-C/S to represent the control sample.

Characterization

XRD measurements were carried out on a Bruker D8 X-ray diffractometer with Cu K α radiation ($\lambda = 1.5405 \text{ \AA}$) in the scan range of 10°-70°. Raman spectra were obtained using a Renishaw inVia micro-Raman spectroscopy system. The morphology of the as-prepared samples was characterized by using a scanning electron microscope (FE-SEM, Hitachi, S4800) equipped with energy dispersive X-ray spectroscopy (EDS) and a transmission electron microscope (TEM, JEM 100-CXII, 80 KV). The thermogravimetric analysis (TGA) of MS-C/S was examined by using NETZSCH STA 449C thermo-analyzer in argon atmosphere.

To obtain the electrodes for the electrochemical measurement, we first dispersed MS-C/S, Ketjenblack, CMC and SBR in a weight ratio of 90:5:1.5:3.5 in distilled water, spread them uniformly on an ultrathin carbon paper current collector, and then placed them in vacuum at 55 °C for 10 h. To illustrate the effect of MS-C improving the conductivity of sulfur cathode, we also prepared a control cathode by using the aforementioned procedure but with the MS-C/S replaced by the sublimed sulfur, and we will name this control electrode as K-C/S for convenience. We then assembled the cathode, the counter electrode (pure lithium foil), the electrolyte [1 M LiTFSI and 0.4 M LiNO₃ in DME/DOL (2 : 1 V/V)], and a Celgard 2400 separator in an argon-filled glove box to obtain coin cells CR2032. The discharge-charge tests were recorded on a Land BT2000 Battery Test System (Wuhan, China). Cyclic voltammetry was carried out on a CHI600D Electrochemical Workshop (Shanghai, China) at a scan rate of 0.1 mV/s to examine the electrochemical reaction of the cell. Electrochemical impedance spectroscopy (EIS) was performed on the coin cell with

an IM6e electrochemical station with an applied sinusoidal excitation voltage of 5 mV in a frequency range from 50 mHz to 1 MHz.

Results and discussion



Scheme 1. Schematic illustration of the synthesis process of the MS-C/S

We first give a brief description of the synthesis process of the MS-C/S, which is environmentally friendly, convenient and low cost. As shown in Scheme 1, the porous MS-C was fabricated by a spray drying of MWCNTs aqueous dispersion; the sublimed sulfur was then mixed with the MS-C uniformly in carbon disulfide under constant stirring. After the slow evaporation of the carbon disulfide, the mixture was sealed in a glass tube and heated at 155 °C for 12 h.

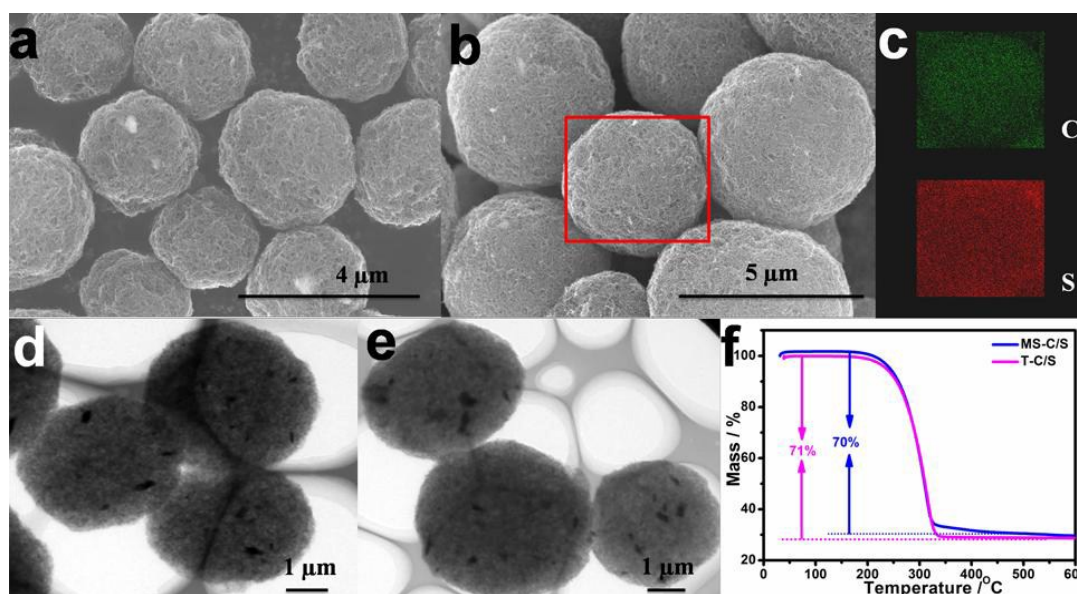


Fig. 1 SEM images of (a) the porous MS-C and (b) the MS-C/S; (c) corresponding element maps of carbon and sulfur for the red rectangular region shown in (b); TEM images of (d) the MS-C and (e) the MS-C/S; (f) TGA results of the MS-C/S and T-C/S.

The morphology of the porous MS-C and the MS-C/S samples were examined by a scanning electron microscope (SEM) and a transmission electron microscope (TEM). The SEM image of the MS-C (Fig. 1a) reveals that numerous MWCNTs intertwine together and form a homogeneous microspherical structure with particle size of several micrometers. The rough surface of the MS-C indicates the polyporous architecture is beneficial for loading sulfur. Fig. S1 shows the SEM images of single MWCNTs microspheres before and after heat treatment at 600 °C in Ar atmosphere. After calcination,

the surface of the microspheres becomes denser without any other change, which means the structure displays good thermal stability. When encapsulating sulfur into the microspheres, the surface of the MS-C/S (Fig. 1b) becomes smoother than that of the pure carbon matrix (Fig. 1a), while the particle size and the morphology remain the same. This implies that sulfur is composited well with the MS-C. The corresponding energy dispersive X-ray spectroscopy (EDS) elemental maps of the MS-C/S are shown in Fig. 1c. The EDS maps prove the existence of sulfur in the carbon matrix, and the consistent signal suggests the distribution of the sulfur is uniform. The TEM images in Fig. 1d and 1e further confirm the existence of a polyporous microspherical architecture. In such an architecture, the MWCNTs are well interconnected to build continuous electronic conductive networks, which improve the conductivity of the sulfur cathode and maintain the integrity of the cathode during the cycling process. Furthermore, the porous structure makes the electrolyte easy to infiltrate into a thick active material layer and react with the interior sulfur.

Thermogravimetric analysis (TGA) was performed in an argon environment to determine the sulfur content. Fig. 1f shows that the content of sulfur in the MS-C/S is 70 wt%. When the sulfur content increases to 77 wt% (Fig. S2), the microspheres are agglomerated and the particle size becomes inhomogeneous (Fig. S2). Hence, the sulfur content of 70 wt% is appropriate for the MS-C/S.

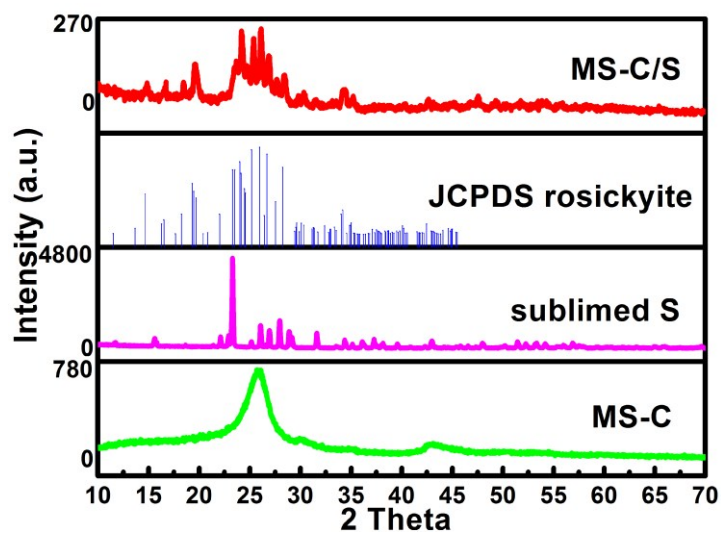


Fig. 2 XRD spectra of the MS-C, sublimed sulfur and MS-C/S.

The X-ray diffraction (XRD) patterns of the MS-C, sublimed sulfur and MS-C/S are shown in Fig. 2. For sublimed sulfur, the sharp and strong diffraction peaks indicate a well-defined crystalline S_8 phase.³⁶ After sulfur impregnated, the sulfur in the MS-C/S turns to rosickyite (JCPDS card No. 01-071-0137), which is an allotrope of S_8 . Compared with the original S_8 , the intensity of S is receded obviously, which suggests that the sulfur is now deeply embedded into the MWCNTs microspheres and well dispersed in the carbon matrix. Note that before thermal treatment the sulfur in the C/S composite is also in S_8 phase (Fig. S4). The interaction between the sublimed sulfur and the dispersant in the MWCNTs aqueous dispersion during the melt-diffusion process may lead to the change of the crystal structure. However, this needs to be verified.

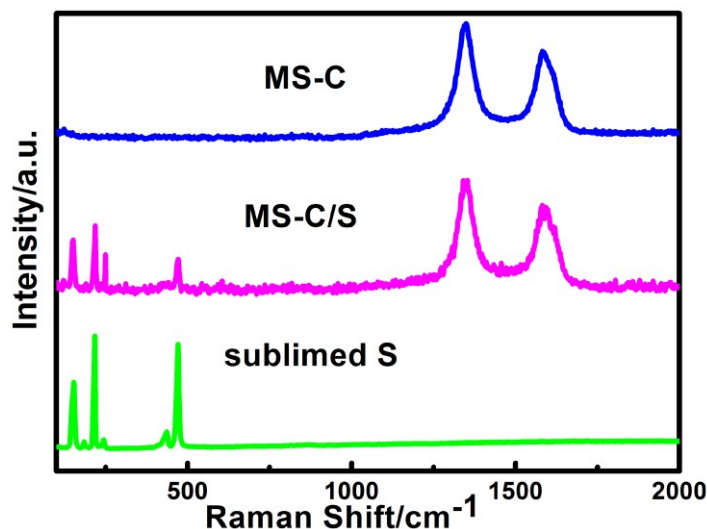


Fig. 3 Raman spectra of the MS-C, sublimed sulfur and MS-C/S.

The Raman spectra of the MS-C, sublimed sulfur, and MS-C/S are plotted in Fig. 3. The spectrum of the MS-C shows two strong peaks at 1585 cm^{-1} (G-band) and 1350 cm^{-1} (D-band), respectively. The G peak corresponds to the graphitic cluster lattice vibration mode with E_{2g} symmetry, and the D peak is activated by the disordered carbon.³⁵ The pure sulfur has several strong vibrational signals below 500 cm^{-1} ; however, for the sulfur in the MS-C/S, these signals are much weaker (without any other noticeable differences).

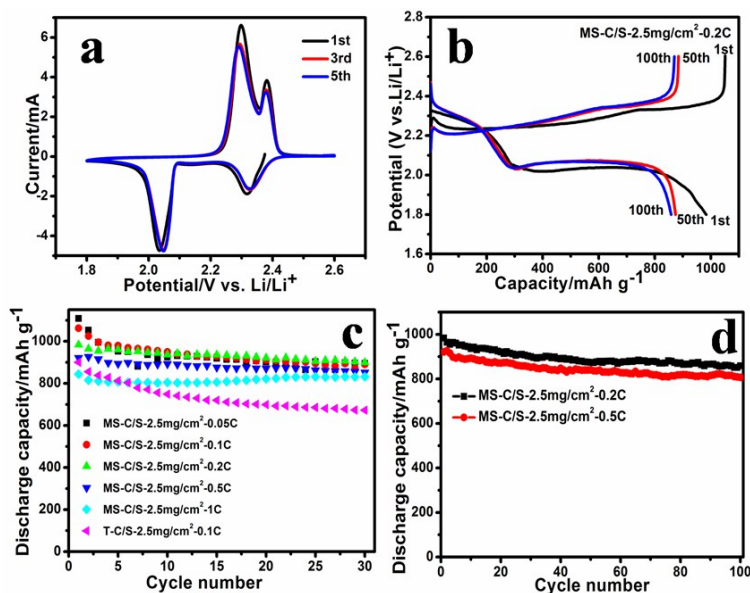


Fig. 4 (a) Cyclic voltammograms of the MS-C/S electrodes at a scan rate of 0.1 mV/s in the voltage range of $1.8\text{--}2.8\text{ V}$; (b) The 1st, 50th, and 100th galvanostatic discharge/charge curves of the MS-C/S electrodes with 2.5 mg/cm^2 sulfur loading at a current rate of 0.2 C in the voltage range of $1.8\text{--}2.6\text{ V}$ versus Li^+/Li ; (c) The discharge capacity versus the cycle number of the MS-C/S electrodes at various current rates (0.05 C , 0.1 C , 0.2 C , 0.5 C and 1 C), compared with the T-C/S electrodes at a rate of 0.1 C ; (d) Cycling performance of the MS-C/S electrodes at a current rate of 0.2 C and 0.5 C . The capacity is calculated based on the mass of the sulfur active material in the MS-C/S.

The electrochemical performance of the MS-C/S was tested by cyclic voltammetry

(CV) and galvanostatic discharge/charge cycling. The electrochemical reaction of the rosenite is the same as that of typical S_8 . Fig. 4a shows the representative CV curves of the MS-C/S electrodes during lithiation/delithiation process. Two cathodic peaks at 2.32 and 2.05 V are observed, which can be attributed to the reduction of sulfur to soluble polysulfide intermediate and insoluble low-order S^{2-} . Meanwhile, the anodic peaks at 2.3 and 2.38 V indicate the oxidation of lithium sulfides to polysulfide and element sulfur.³⁷ These four peaks are reversible in the reduction and oxidation processes, which reveals the good stability of the MS-C/S electrodes; the reversibility is due to the microspherical structure with effective 3D mixed conducting networks.

Fig. 4b presents the discharge/charge profiles of the MS-C/S electrodes with 2.5 mg cm^{-2} sulfur loading at a current rate of 0.2 C. There are also two obvious cathodic and two anodic plateaus, which demonstrate typical sulfur cathode charge/discharge behavior and agree well with previous CV curves.^{38,39} The MS-C/S electrode shows an initial discharge capacity of 983 mA h g^{-1} , and the capacity gradually decays to 874 mA h g^{-1} in the first 50 cycles (Fig. 4b). A stable capacity of about 858 mA h g^{-1} (87% of the initial capacity) remains until 100 cycles. The irreversible dissolution of polysulfide into electrolyte and the redistribution of sulfur result in the decrease of the capacity, while the following stabilized electrochemical performance can be attributed to the strong adsorption ability of MWCNTs microspheres, which capture the polysulfide effectively.⁴⁰

The rate capability of the MS-C/S electrodes with sulfur loading of 2.5 mg cm^{-2} at different current rates (0.05 C-1 C) is shown in Fig. 4c. The reversible discharge capacities of the first cycle are 1108, 1062, 983, 921 and 844 mA h g^{-1} at constant current rates of 0.05 C, 0.1 C, 0.2 C, 0.5 C and 1 C, respectively. After 30 cycles, the capacities gradually reduce to 895, 891, 900, 852 and 831, respectively. Compared with the initial capacity, the capacity retentions of the 30th cycle at 0.05 C, 0.1 C, 0.2 C, 0.5 C and 1 C are 81%, 84%, 91%, 93% and 98.4%, respectively. The MS-C/S electrode shows an excellent rate stability. In long-term cycling, the MS-C/S electrode remains a high discharge capacity of 858 mA h g^{-1} over 100 cycles at the current rate of 0.2 C (Fig. 4d). Besides, the MS-C/S electrode delivers a reversible capacity of 806 mA h g^{-1} after 100 cycles, with a high capacity retention of 88%, even at 0.5 C.

For comparison, a control sample (T-C/S) was prepared by melt-diffusion of pure MWCNTs and sulfur. Its sulfur content is measured to be 71% (see Fig. 1f), which is quite close to that of the MS-C/S. As shown in Fig. 4c, the T-C/S with the same sulfur loading shows an initial capacity of 900 mA h g^{-1} , and a reversible capacity about 672 mA h g^{-1} after 30 cycles at 0.1 C, whose capacity retention (75%) is much lower than the MS-C/S electrode.

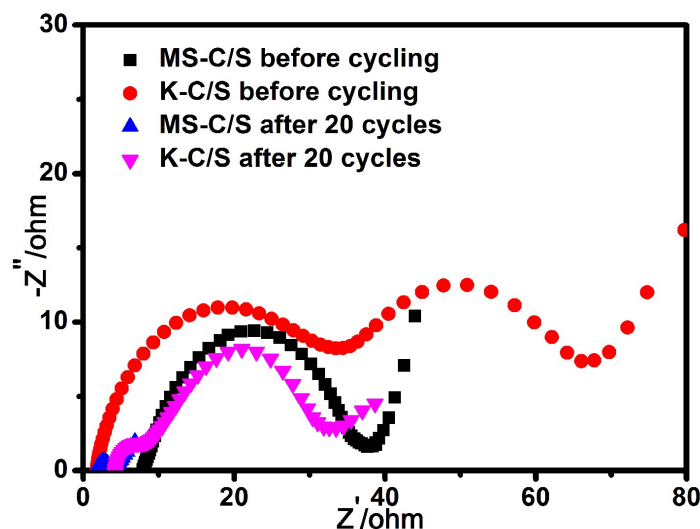


Fig. 5 Electrochemical impedance spectra of the MS-C/S and K-C/S before and after 20 cycles at 0.1 C

Fig. 5 shows the EIS spectra of the MS-C/S and K-C/S electrodes before and after cycling for 20 cycles. The diameter of the depressed semicircle in the high frequency region is regarded as the charge transfer resistance (R_{ct}) of the cell. According to the fitting of the equivalent circuit, before cycling, the R_{ct} of MS-C/S and K-C/S cells is 30.4 Ohm and 49.4 Ohm, respectively. The lower charge transfer resistance of MS-C/S electrode could be attributed to the much-enhanced conductivity of the MS-C/S cathode. Moreover, the R_{ct} of the MS-C/S electrode is reduced to 1.9 Ohm after 20 cycles, while that of the K-C/S remains at 32.6 Ohm.

In addition, the morphology of the MS-C/S electrode before and after 20 cycles at 0.1 C is shown in Fig. S5. Even after 20 cycles (Fig. S5b), the particles on the electrode are still well-dispersed microspheres without obvious change in the morphology, which further confirms the stability of the microspheres architecture and the well infiltration of sulfur into the carbon framework.

Conclusion

In summary, a novel type of multi-walled carbon nanotubes microspheres were prepared and applied to the sulfur cathode of lithium sulfur batteries. The MWCNTs microspheres were fabricated through a simple one-step spray drying of MWCNTs aqueous dispersion. The resulted carbon framework shows an homogeneous polyporous microspherical architecture with particle size around several micrometers. The MWCNTs in the microspheres are well interconnected and form a 3D continuous electronic conductive network. When applied to the Li-S batteries, the element sulfur infiltrates into the MWCNTs microspheres uniformly, and the carbon matrix then immobilizes the polysulfide efficiently and prevents their diffusion into the electrolyte to minimize the shuttling effect. In the meanwhile, the porous structure is also beneficial for the quick infiltration of liquid electrolyte and makes it easy to react with the interior sulfur. Furthermore, the carbon skeleton is not only a predominant reservoir for polysulfide intermediate, but also an efficient buffer to alleviate the volume expansion/shrinkage during the charge and discharge process. Thus, the MS-C/S electrodes exhibit excellent

electrochemical performance. Typically, at a high current rate of 0.5 C, the MS-C/S electrodes deliver a reversible capacity of 806 mA h g⁻¹ after 100 cycles with 88% capacity retention. All these results suggest that such carbon framework with efficient 3D conductive network prepared by a facile approach using low cost raw material is promising for the practical application in energy storage and conversion devices such as sodium-ion batteries, lithium-ion batteries or fuel cells.

Acknowledgements

This work was supported by the Natural Science Foundation of China (Grant No. 51222210, 51472268, 11234013), the “973” Projects (2012CB932900), the Strategic Priority Research Program of the Chinese Academy of Sciences (XDA09010300) and the Hundred-Talent Program of the Chinese Academy of Sciences.

Notes and references

1. K. Ding, Y. Bu, Q. Liu, T. Li, K. Meng and Y. Wang, *J. Mater. Chem. A*, 2015, 3, 8022-8027.
2. L. Suo, Y. S. Hu, H. Li, M. Armand and L. Chen, *Nature communications*, 2013, 4, 1481.
3. M. K. Song, E. J. Cairns and Y. Zhang, *Nanoscale*, 2013, 5, 2186-2204.
4. W. Zhou, Y. Yu, H. Chen, F. J. DiSalvo and H. D. Abruna, *Journal of the American Chemical Society*, 2013, 135, 16736-16743.
5. C. Wang, W. Wan, J.-T. Chen, H.-H. Zhou, X.-X. Zhang, L.-X. Yuan and Y.-H. Huang, *J. Mater. Chem. A*, 2013, 1, 1716-1723.
6. H. Chen, C. Wang, W. Dong, W. Lu, Z. Du and L. Chen, *Nano letters*, 2015, 15, 798-802.
7. L. Fei, X. Li, W. Bi, Z. Zhuo, W. Wei, L. Sun, W. Lu, X. Wu, K. Xie, C. Wu, H. L. Chan and Y. Wang, *Advanced materials*, 2015, DOI: 10.1002/adma.201502668.
8. Z. Li, S. Zhang, C. Zhang, K. Ueno, T. Yasuda, R. Tatara, K. Dokko and M. Watanabe, *Nanoscale*, 2015, 7, 14385-14392.
9. Z. L. Wang, D. Xu, J. J. Xu and X. B. Zhang, *Chemical Society reviews*, 2014, 43, 7746-7786.
10. G. Xu, B. Ding, L. Shen, P. Nie, J. Han and X. Zhang, *Journal of Materials Chemistry A*, 2013, 1, 4490.
11. L. Xiao, Y. Cao, J. Xiao, B. Schwenzer, M. H. Engelhard, L. V. Saraf, Z. Nie, G. J. Exarhos and J. Liu, *Advanced materials*, 2012, 24, 1176-1181.
12. Q. Pang, J. Tang, H. Huang, X. Liang, C. Hart, K. C. Tam and L. F. Nazar, *Advanced materials*, 2015, DOI: 10.1002/adma.201502467.
13. J. Wang, C. Lv, Y. Zhang, L. Deng and Z. Peng, *Electrochimica Acta*, 2015, 165, 136-141.
14. C. Wang, H. Chen, W. Dong, J. Ge, W. Lu, X. Wu, L. Guo and L. Chen, *Chemical communications*, 2014, 50, 1202-1204.
15. T. Xu, J. Song, M. L. Gordin, H. Sohn, Z. Yu, S. Chen and D. Wang, *ACS Applied Materials & Interfaces*, 2013, 5, 11355-11362.
16. Y. Zhou, C. Zhou, Q. Li, C. Yan, B. Han, K. Xia, Q. Gao and J. Wu, *Advanced materials*, 2015, 27, 3774-3781.
17. Y. Chen, S. Lu, X. Wu and J. Liu, *The Journal of Physical Chemistry C*, 2015, 119, 10288-10294.
18. X. Liang, Z. Wen, Y. Liu, H. Zhang, J. Jin, M. Wu and X. Wu, *Journal of Power Sources*, 2012, 206, 409-413.
19. Y. Huang, M. Zheng, Z. Lin, B. Zhao, S. Zhang, J. Yang, C. Zhu, H. Zhang, D. Sun and Y. Shi, *J. Mater. Chem. A*, 2015, 3, 10910-10918.
20. H. Hu, H. Cheng, Z. Liu, G. Li, Q. Zhu and Y. Yu, *Nano letters*, 2015, 15, 5116-5123.
21. J. H. Kim, K. Fu, J. Choi, K. Kil, J. Kim, X. Han, L. Hu and U. Paik, *Scientific reports*, 2015, 5, 8946.

22. N. Moreno, M. Agostini, A. Caballero, J. Morales and J. Hassoun, *Chemical communications*, 2015, DOI: 10.1039/c5cc05162b.
23. M. A. Pope and I. A. Aksay, *Advanced Energy Materials*, 2015, 5, 1500124.
24. J. Xiao, *Advanced Energy Materials*, 2015, 5, 1501102.
25. Y. S. Su, Y. Fu, T. Cochell and A. Manthiram, *Nature communications*, 2013, 4, 2985.
26. W. Zhou, C. Wang, Q. Zhang, H. D. Abruña, Y. He, J. Wang, S. X. Mao and X. Xiao, *Advanced Energy Materials*, 2015, 5, 1401752.
27. S.-R. Chen, Y.-P. Zhai, G.-L. Xu, Y.-X. Jiang, D.-Y. Zhao, J.-T. Li, L. Huang and S.-G. Sun, *Electrochimica Acta*, 2011, 56, 9549-9555.
28. Z. Peng, W. Fang, H. Zhao, J. Fang, H. Cheng, T. N. L. Doan, J. Xu and P. Chen, *Journal of Power Sources*, 2015, 282, 70-78.
29. X. Tao, X. Chen, Y. Xia, H. Huang, Y. Gan, R. Wu, F. Chen and W. zhang, *Journal of Materials Chemistry A*, 2013, 1, 3295.
30. G. Zheng, Q. Zhang, J. J. Cha, Y. Yang, W. Li, Z. W. Seh and Y. Cui, *Nano letters*, 2013, 13, 1265-1270.
31. J. He, Y. Chen, P. Li, F. Fu, Z. Wang and W. Zhang, *J. Mater. Chem. A*, 2015, 3, 18605-18610.
32. L. Sun, W. Kong, Y. Jiang, H. Wu, K. Jiang, J. Wang and S. Fan, *J. Mater. Chem. A*, 2015, 3, 5305-5312.
33. R. Chen, T. Zhao, J. Lu, F. Wu, L. Li, J. Chen, G. Tan, Y. Ye and K. Amine, *Nano letters*, 2013, 13, 4642-4649.
34. J. Guo, Y. Xu and C. Wang, *Nano letters*, 2011, 11, 4288-4294.
35. J. Ma, Z. Fang, Y. Yan, Z. Yang, L. Gu, Y.-S. Hu, H. Li, Z. Wang and X. Huang, *Advanced Energy Materials*, 2015, 5, 1500046.
36. J. Ye, F. He, J. Nie, Y. Cao, H. Yang and X. Ai, *J. Mater. Chem. A*, 2015, 3, 7406-7412.
37. C. Wu, L. Fu, J. Maier and Y. Yu, *J. Mater. Chem. A*, 2015, 3, 9438-9445.
38. Y. Son, J.-S. Lee, Y. Son, J.-H. Jang and J. Cho, *Advanced Energy Materials*, 2015, 5, 1500110.
39. M. Yu, R. Li, Y. Tong, Y. Li, C. Li, J.-D. Hong and G. Shi, *J. Mater. Chem. A*, 2015, 3, 9609-9615.
40. R. Singhal, S.-H. Chung, A. Manthiram and V. Kalra, *J. Mater. Chem. A*, 2015, 3, 4530-4538.